ACS OMEGA

Article

Cite This: ACS Omega 2018, 3, 16542−16548

http://pubs.acs.org/journal/acsodf

# Polyvinylbutyral−Polyaniline Nanocomposite for High Microwave Absorption Efficiency

Pritom J. Bora,[†] Irthasa Azeem,[‡] K. J. Vinoy,[§] Praveen C. Ramamurthy,*[,†,‡] and Giridhar Madras[†]

[†]Interdisciplinary Centre for Energy Research (ICER), [‡]Department of Materials Engineering, and [§]Department of Electrical and Communication Engineering, Indian Institute of Science, Bangalore 560012, India

Supporting Information

**ABSTRACT:** A coatable polyvinylbutyral (PVB)−polyaniline (PANI) nanocomposite was designed for high microwave absorption efficiency. The maximum absorption efficiency 88.2 dB GHz/mm was obtained for the PANI nanofiber-loaded PVB (PVBPN) nanocomposite with a large bandwidth, whereas a pristine PANI-containing composite shows 53.5 dB GHz/mm in the frequency range 8.2−18 GHz. The presence of nanoslit pores in PVBPN also helps to achieve a large bandwidth and hence high microwave absorption efficiency. Standard electromagnetic simulation also shows that power absorbed by the PVBPN nanocomposite is high and its ultrathin coating over the dielectric substrate (epoxy) is promising for broadband tuneable reflection loss.

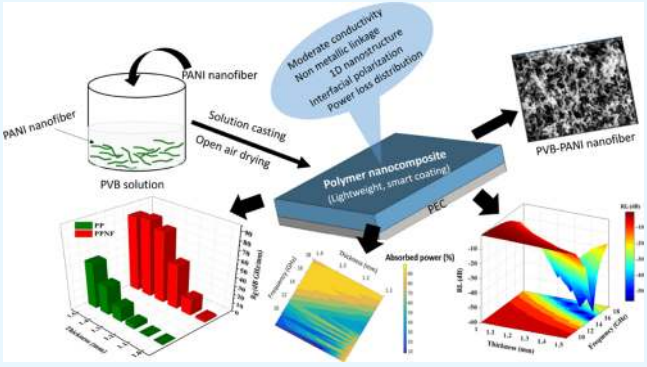


## INTRODUCTION

Recent interest is on lightweight broadband ultrathin microwave absorbing materials.[1−4] The lightweight and broadband microwave absorption property of a single layer material is understood from the microwave absorption efficiency.[5−8] Nonmetallic/composite materials are well known for microwave absorption along with metamaterials.[1,2,4,9,10] Lightweight, ultrathin coatable polymer nanocomposites for microwave absorption especially in high frequency (8.2−18 GHz) have attracted interest recently to protect from electromagnetic (EM) threats such as EM interference (EMI).[11−13] Furthermore, there are many advantages of using polymer nanocomposites for microwave absorption such as corrosion protective, large area fabrication, inexpensive, and so forth.[14] The conventional ferrite-based absorbers such as nickel, cobalt, nickel−zinc, cobalt−zinc ferrites were designed based on the impedance matching and suggesting that the magnetic dielectric core−shell structure is promising.[15−21] The EM absorbers such as reduced graphene oxide−ferrite and carbon nanotubes−ferrites were also designed in a similar manner.[22−26] Recently, morphology tuning of dielectrics for broadband microwave absorption has been proposed.[27,28] The conducting polymers, especially polyaniline (PANI)-based materials, were also reported for microwave absorption.[29−31] The significant importance received by PANI for microwave absorption is due to the adjustable conductivity, permittivity value, molecular weight, and bulk-level easy synthesis.[32,33] Further, the morphology of PANI can be easily tuned and easy to disperse in the polymer matrix. Apart from this, PANI is proposed for smart coating because of its self-healing properties.[34,35]

The conductivity of PANI can be easily adjusted depending on synthesis conditions.[32] Low-temperature (−30 ± 2 °C) PANI synthesis results high molecular weight and is also reported for high conductivity.[32] Huang and Kaner report that the bulk amount of PANI nanofiber (PNF) can be easily synthesized in one-step chemical synthesis at room temperature.[36] A PANI-loaded weather resistive polymer such as polyvinylbutyral (PVB)/polyurethane/epoxy is reported for EMI shielding application.[31,33,37] The key interest on PVB is that it is more attractive for packaging/encapsulation as well as smart coating especially in organic electronics.[38] The objective of the present work is to design ultrathin polymer nanocomposites (PVB−PANI) based on material properties for high microwave absorption efficiency.

## DESIGN APPROACH

In general, the microwave absorbing materials are designed for the metal/perfect electric conductor (PEC) backed condition. The reflection loss (RL) of a single layer absorber is given by[1−5]

$$\text{Reflection loss (RL)} = 20 \log \left| \frac{Z_{in} - Z_0}{Z_{in} + Z_0} \right| (\text{dB}) \quad (1)$$

Received: August 14, 2018
Accepted: October 29, 2018
Published: December 4, 2018






DOI: 10.1021/acsomega.8b02037
ACS Omega 2018, 3, 16542−16548

$Z_{in}$ = input impedance and it can be written as

$$Z_{in} = (\mu_0\mu_r/\varepsilon_0\varepsilon_r)^{1/2} \tanh[j2\pi fd(\mu_0\mu_r/\varepsilon_0\varepsilon_r)^{1/2}] \quad (2)$$

$Z_0$ is the characteristic impedance of free space (=377) and $d$ = thickness of the absorber.

$\varepsilon_r$ and $\mu_r$ are relative permittivity ($\varepsilon_r = \varepsilon' - i\varepsilon''$) and permeability ($\mu_r = \mu' - i\mu''$), respectively.

For practical applications, the RL value of −10 dB is the optimum level (corresponds to 90% absorption), and therefore, microwave absorption efficiency ($R_E$) of a material is expressed as[5−8]

$$R_E = \frac{\Delta S}{d} \quad (3)$$

where $\Delta S = \int \mathrm{RL} df_{\mathrm{RL}\leq -10\mathrm{dB}}$.

The $R_E$ value depends on thickness, bandwidth (RL ≤ −10 dB), and minimum RL value. For better microwave absorption efficiency, large bandwidth with a minimum RL value and low thickness is preferred.[2] The literature shows that for large bandwidth and a minimum RL value, the moderate electrical conductivity of the absorbing layer and uniform power loss distribution is advantageous. According to the free electron theory, the electrical conductivity is given by[9] $\sigma = \pi\varepsilon_0 f\varepsilon''$. Further, the permittivity value should not be very high to achieve high bandwidth. This is because the derivative of $Z_{in}$ with respect to $d(\partial Z_{in}/\partial d)$ can be expressed as[39]

$$\frac{\partial Z_{in}}{\partial d} = \frac{j2\pi f\mu_0(\mu' - j\mu'')}{[\cosh(j2\pi f\sqrt{\varepsilon_0\mu_0(\varepsilon' - i\varepsilon'')(\mu' - j\mu'')}\, d]^2} \quad (4)$$

Thus, it also indicates that for low permittivity, $\partial Z_{in}/\partial d$ is high and RL is sensitive to the thickness.

The one-dimensional dielectric nanofiller (rod, fiber) is advantageous for better microwave absorption, as they can form the linkage easily inside the matrix which leads to the interfacial polarization as well as effective permittivity along with the dielectric loss. The isotropic antenna mechanism also plays a key role for rod or fiber nanostructures.[28,40] According to that, the dielectric nanorods/nanofibers can act as a receiver antenna for incident energy and transform it into the small dissipative current (micro current) through it.[28] On the basis of the above mentioned factors, the PVB−PNF composite was designed and is schematically shown in Figure 1. In our previous work,[2] the RL value of the PVB−PANI nanocomposite (PNF synthesized at 25 °C) was reported for a thick single layer (≥2 mm).[2] However, the microwave absorption efficiency of the PVB−PANI nanocomposite (PNF synthesized at ∼0 °C) and its coating on lightweight structural materials such as epoxy for microwave absorption were not investigated. Present effort attempts to investigate the PVB−PNF (synthesized at ∼0 °C) coated epoxy composite for microwave absorption.

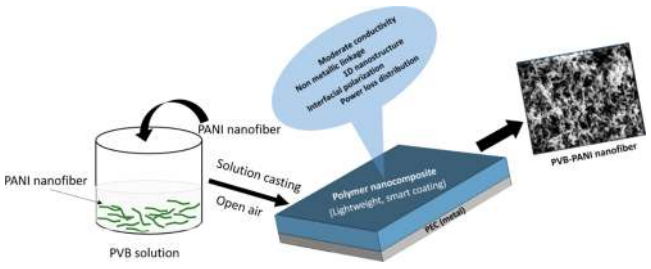


**Figure 1.** Schematic of the designed polymer nanocomposite for high microwave absorption efficiency and its simple fabrication.

## RESULTS AND DISCUSSION

The cross-sectional surface morphology of the as-prepared PPNF nanocomposite is shown in Figure 2a (low magnification) and Figure 2b (high magnification). It suggests that PNFs (average diameter ∼50 nm and length ∼1 μm) form a network in the PVB. However, a few nanoslit pores were also observed.

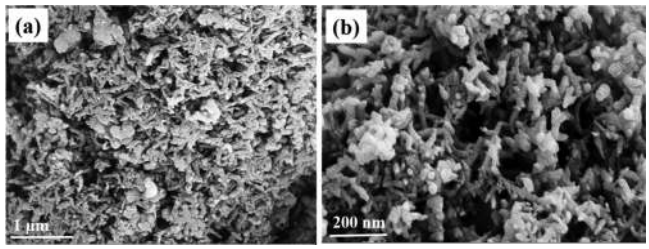


**Figure 2.** Cross-sectional surface morphology of the as-prepared PPNF nanocomposite film at (a) low magnification and (b) high magnification.

Figure 3a,b respectively shows the variation of real ($\varepsilon'$) and imaginary part ($\varepsilon''$) of the permittivity of PPNF and PP composites in the frequency range 8.2−18 GHz. The $\varepsilon'$ corresponds to the storage ability of electric energy, whilst $\varepsilon''$ correspond to the dissipation of electric energy. As observed in Figure 3a,b, $\varepsilon'$ value of PPNF nanocomposite (13.5−12) is higher than the PP composite (8.5−8). Hence, it indicates the high storage ability of electric field energy by PPNF. Similarly, the $\varepsilon''$ value of PPNF is also higher than the PP composite (Figure 3b), indicating higher electric energy dissipation in PPNF compared to the PP composite. Mechanistically, the obtained high value of $\varepsilon'$ and $\varepsilon''$ of PPNF as compared to the PP composite is due to the interfacial polarization, heterogeneity, as well as morphology. As the surface to volume ratio of PNFs is high, the presence of it in PVB leads to more heterogeneity as well as effective permittivity and the interfacial polarization, which can be identified from the change of the $\varepsilon''$ value, that is, $\Delta\varepsilon''$.[42] The $\Delta\varepsilon''$ value of the PPNF nanocomposite is 1.1, which is much higher than that of the PP composite (0.6), indicating that interfacial polarization in the PPNF nanocomposite is more as compared to that in the PP composite in the 8.2−18 GHz range.[42,43] It is believed due to the much heterogeneous interfaces in the PPNF nanocomposite (as the PANI nanofiber creates more linkage inside the PVB) as compared to the PP composite.

The thickness-dependent RL (dB) values of PPNF and PP composites are shown in Figure 4a,b, respectively. As shown in Figure 4a, the minimum RL value −14.7 dB was obtained for the PPNF nanocomposite (1 mm), while the minimum RL value of the PP composite was obtained as −5 dB for the same thickness. On increasing the thickness by 0.1 mm, the RL value of the PPNF nanocomposite was decreased with a wide bandwidth and owing to one-fourth wavelength equation, that is[17,19,21]

$$d_m = \frac{n\lambda}{4} = \frac{nc}{4f_m[(|\varepsilon_r||\mu_r|)]^{1/2}} \qquad (n = 1,\ 3,\ 5,\ \ldots) \quad (5)$$



DOI: 10.1021/acsomega.8b02037
ACS Omega 2018, 3, 16542−16548

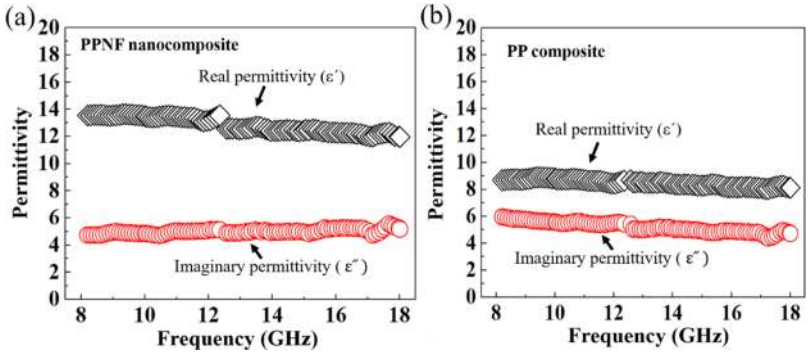


**Figure 3.** Variation of real permittivity ($\varepsilon'$) and imaginary permittivity ($\varepsilon''$) values of (a) PPNF and (b) PP composite in 8.2−18 GHz.

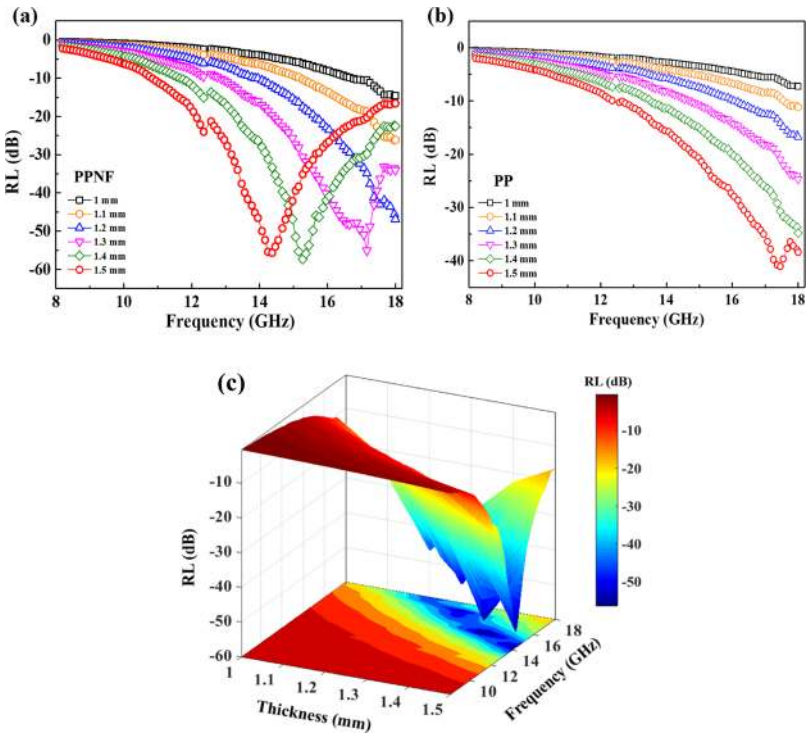


**Figure 4.** Thickness-dependent RL (dB) of (a) PPNF nanocomposite, (b) PP composite, and (c) three-dimensional (3D) plot of the PPNF nanocomposite in the 8.2−18 GHz range.

Here, $d_m$ and $f_m$ are the matching thickness and the matching frequency, respectively, with respect to the RL peak. From eq 5, it is clear that the shift of the RL peak to the lower frequency region occurs by increasing the absorber thickness. The minimum RL values of the PPNF nanocomposite were −46.5, −55.5, −57.4, and −55.7 dB for the thicknesses 1.2, 1.3, 1.4, and 1.5 mm, respectively. On the other hand, the minimum RL value was obtained as −43 dB for the PP composite (1.5 mm). To determine the $R_E$ value, bandwidth ($f_E$) and corresponding area were calculated for the PPNF nanocomposite. As shown in Figure 5a−d, the obtained $f_E$ values of PPNF nanocomposites were found to be 4.2, 5.7, 6.1, and 7.3 GHz, respectively. The $R_E$ values of the PPNF nanocomposite were found to be 18.3, 50.4, 81.1, 88.2, and 86 dB GHz/mm for the thickness 1.1, 1.2, 1.3, 1.4, and 1.5 mm respectively. On the other hand, the maximum $R_E$ value was found to be 52.3 dB GHz/mm for the PP composite for the thickness 1.5 mm. The comparison of the $R_E$ value with thickness for the PPNF nanocomposite and the PP composite is shown in Figure 6, and it indicates the excellent microwave absorption efficiency of the PPNF nanocomposite as compared to the PP composite. A comparison of the maximum $R_E$ value of recently engineered composite materials, based on the structure−property relationship, with present composite, is shown in Figure 7. Relatively, PPNF has high a $R_E$ value as compared to the other reported composites. However, the minimum RL value of PPNF can be tuned with thickness, and the minimum RL value can be reached (−79 dB for the thickness 2.5 mm for narrow bandwidth), which decreases the microwave absorption efficiency. In the case of PPNF, the optimal microwave absorption efficiency was achieved for 1.4 mm (Figure 6). Thus, it indicates that thin single layer PPNF coating over dielectrics could be promising to achieve high microwave absorption efficiency, large bandwidth as well as minimum RL.

For a better understanding of outstanding microwave absorption efficiency of the PPNF nanocomposite, a standard EM simulation was carried out using CST Microwave Studio. On the basis of the experimental setup, present composite materials were assigned as shown in Figure 8, and 0.5 W was taken as a default stimulated power on the source port. The



DOI: 10.1021/acsomega.8b02037
ACS Omega 2018, 3, 16542−16548

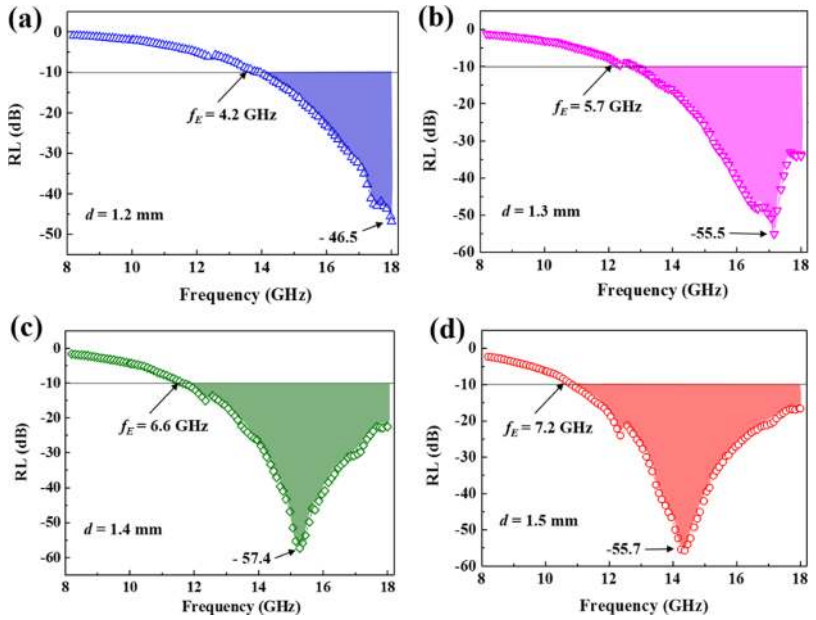


**Figure 5.** RL of the PPNF nanocomposite and with associated parameters for (a) 1.2, (b) 1.3, (c) 1.4, and (d) 1.5 mm.

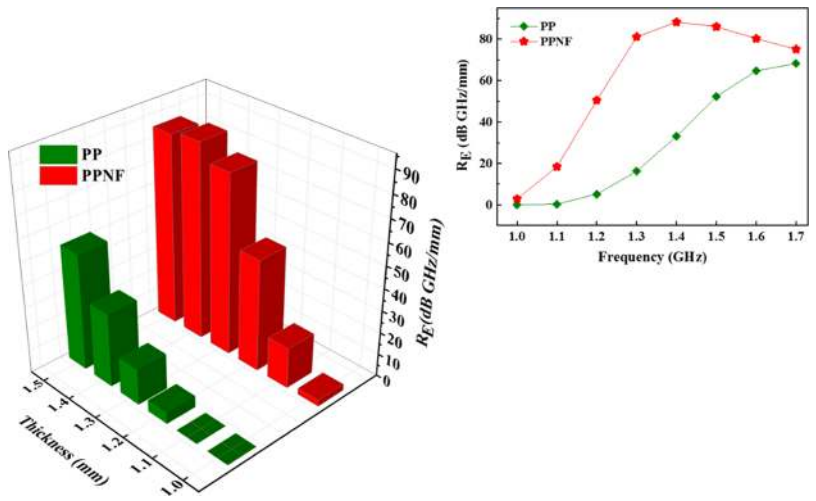


**Figure 6.** Thickness-dependent $R_E$ value of the PPNF nanocomposite and the PP composite in the 8.2−18 GHz range.

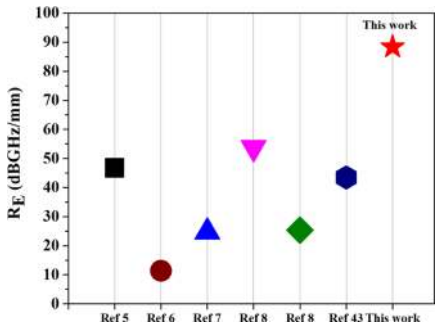


**Figure 7.** Reported maximum microwave absorption efficiency, $R_E$ (dB GHz/mm), of various nanomaterials and the present PPNF nanocomposite (this work).

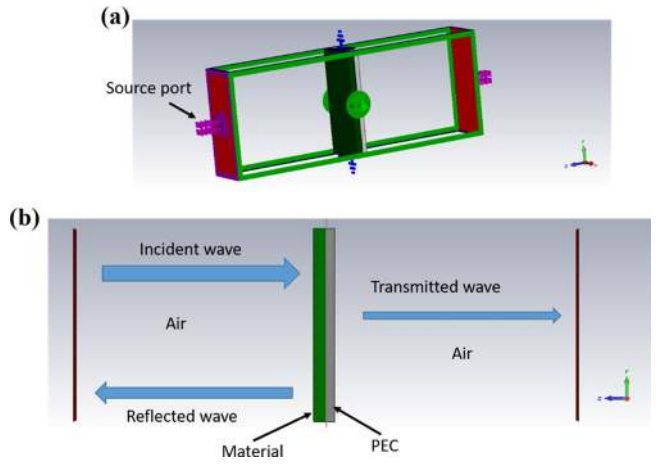


**Figure 8.** Schematic of (a) typical waveguide measurement and (b) absorption composite structure.

obtained absorbed power, reflected power, and loss in metals (PEC) was simulated. The simulated result of the PPNF nanocomposite for different thicknesses is shown in the Figure S1 (Supporting Information). The simulation result indicates



DOI: 10.1021/acsomega.8b02037
*ACS Omega* 2018, 3, 16542−16548

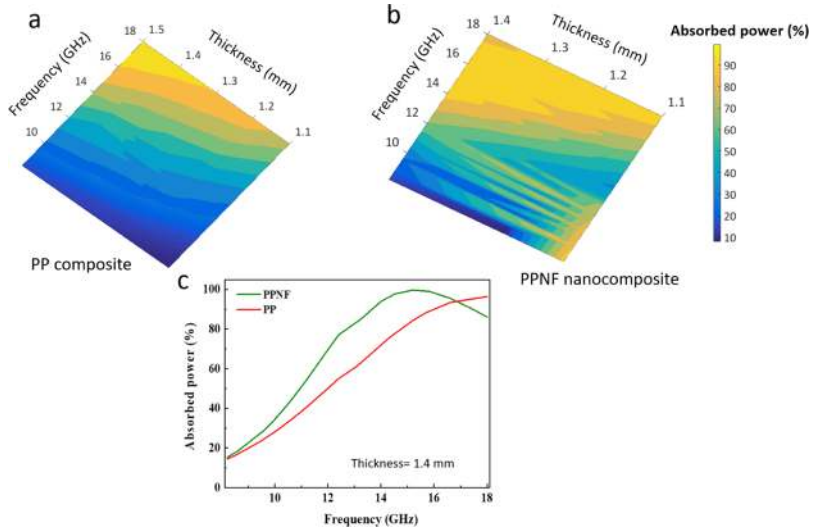


**Figure 9.** Simulated thickness-dependent absorbed power (%) of (a) PP composite and (b) PPNF nanocomposite. (c) Comparison of absorbed power (%) of PPNF and PP composites (thickness 1.4 mm).

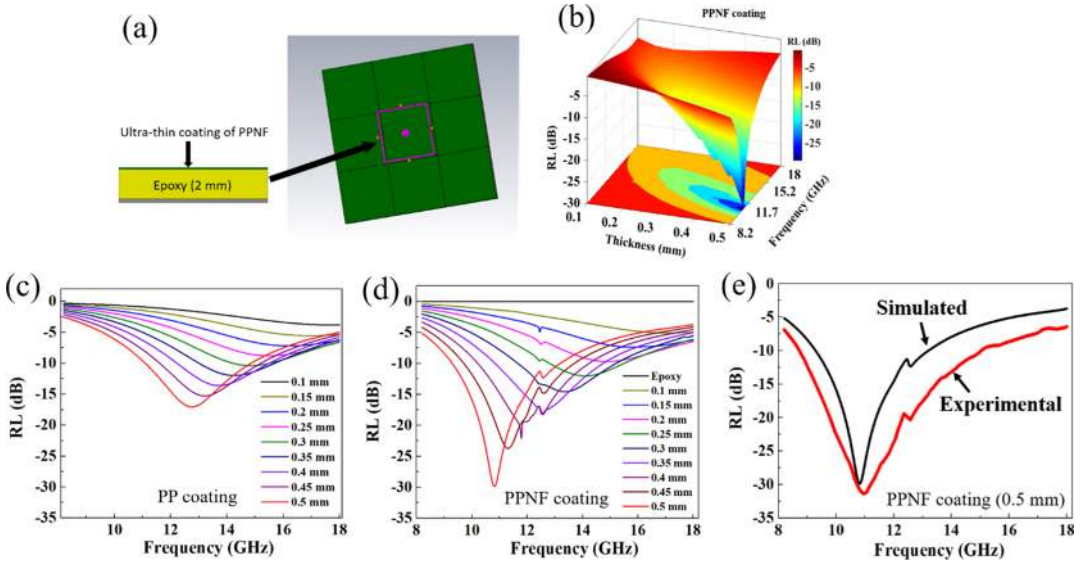


**Figure 10.** (a) Schematic of the PPNF-coated epoxy substrate (2 mm), (b) simulated 3D RL (dB) plot of PPNF-coated epoxy, (c) simulated RL (dB) of various coatings of PP-coated epoxy, and (d) PPNF-coated epoxy. (e) Simulated and experimental RL (dB) of 0.5 mm PPNF nanocomposite-coated epoxy.

that power absorbed by PPNF is predominant in high frequency, and a similar trend is observed in RL. The simulation results of absorbed power and reflected power by the PP composite are shown in Figure S2 (Supporting Information). It shows that power absorbed by the PP composite is much less than the PPNF nanocomposite. The variation of absorbed power (%) by the PP composite and the PPNF nanocomposite in different thicknesses is shown in Figure 9a,b, respectively. As shown in Figure 9a,b, unlike the PPNF nanocomposite, the PP composite cannot absorb all the stimulating power in any frequency for the thickness range 1−1.5 mm. The comparison of absorbed power (%) of the PP composite and the PPNF nanocomposite (thickness 1.4 mm) is shown in Figure 9c, and it clearly indicates the better microwave absorption property of the PPNF nanocomposite as compared to the PP composite.

In the case of the PPNF nanocomposite surface, high power loss takes place. It is because of the presence of PNFs, which act as a receiver antenna for incident microwave and transmit into micro current, and hence, incident power is distributed uniformly inside the PPNF nanocomposite. The effective medium consists of dielectrics and inhomogeneous a few nanoslit pores (the spacing between the two nanofibers). The nanoslit pores act as a tiny transparent plane for incident wave,[44] and therefore, the intrinsically predominant energy loss takes place through the PNFs as nanofibers are well connected in the matrix. Therefore, high power loss distribution can be expected for the PPNF nanocomposite. In other words, the presence of a few nanoslit pores effectively interrupted the spreading of incident microwaves, and hence, dissipation of EM energy takes place owing to the impedance difference, resulting in further enhancement of storage energy and absorption, which also favors achievement of large bandwidth. That is why high microwave absorption efficiency for the PPNF nanocomposite was obtained.



DOI: 10.1021/acsomega.8b02037
ACS Omega 2018, 3, 16542−16548

Mechanistically ultrathin coating of PPNF is advantageous for broad band microwave absorption. The industrial standard polymer which is used most commonly in various applications including aircraft is epoxy. As for most of the applications, 2−3 mm thicker large laminates were preferred; therefore, a simulation of ultrathin PPNF-coated (0.1−0.5 mm) epoxy (2 mm) was carried out in this study. For comparison, the PP composite was also taken. The schematic of the unit cell structure and the artificial periodic array is shown in Figure 10a. In the designed structure, the unit cell with the PEC substrate was constructed with the same area (10 mm × 10 mm) in the periodic array. The boundary conditions, viz., electric and magnetic were applied at the *X*- and *Y*-directions, respectively, so that microwave propagates along the *Z*-axis.

The simulated RL (dB) of PPNF-coated epoxy periodic array is shown in Figure 10a. The RL value was obtained as −25 dB for the PPNF coating 0.4 mm, whereas for 0.2 and 0.3 mm coating, the minimum RL values were obtained as −23, −20, and −10 dB (Figure 10b,d). The minimum RL value was decreased to −29 dB with a large bandwidth for the PPNF coating thickness of 0.5 mm. On the other hand, the minimum RL value was found to be −17.5 dB for PP coating (0.5 mm) over epoxy (Figure 10c). Further, in the case of PP coating, the bandwidth was found to be small, and the standard RL value (−10 dB) was not obtained for the coating thickness up to 0.3 mm. From the simulated RL, it was observed that PPNF ultrathin coating is more advantageous to achieve minimum RL and large bandwidth.

In order to validate the proposed PPNF nanocomposite coating, the epoxy composite was fabricated. Initially, the epoxy laminate (2 mm) was prepared by using commercial epoxy resin (Atul Pvt. Ltd., India), and the PPNF nanocomposite was coated (0.5 mm) on epoxy laminate by solution casting followed by open air drying (24 h) and emery paper polishing. Coating thickness can be controlled through the locally prepared Teflon mould, followed by polishing. The conducting aluminium tape (PEC) was pasted on the back side of the PPNF-coated epoxy, and RL was recorded for 8.2−18 GHz. The experimental and simulated RL of 0.5 mm PPNF-coated epoxy (aluminium backed) is shown in Figure 10e. The tendency of both experimental and simulated RL matches well. In fact, experimental RL covers better bandwidth with the minimum RL value of −32 dB (11 GHz). Thus, it indicates that the PPNF nanocomposite can be considered as one of the potential coating material for tuning the microwave absorption.

## CONCLUSIONS

The coatable polymer nanocomposite was designed and demonstrated for high microwave absorption efficiency. The maximum absorption efficiency of 88.2 dB GHz/mm was obtained for the chemically synthesized PNF-loaded PVB composite with a large bandwidth in the frequency range 8.2−18 GHz. The EM simulation also shows that PNF-loaded PVB has better microwave absorption power as compared to the bulk PANI. Further, the simulation result indicates that an ultrathin coating of the PVB−PANI nanocomposite over the epoxy substrate (2 mm) is promising for tuneable broad band microwave absorption.

## EXPERIMENTAL SECTION

The PNFs were synthesized at 0 ± 1 °C, according to the standard procedure described in the literature (for organic phase chloroform was used and HCl was added in the aqueous phase).[36] For comparison, bulk PANI was also synthesized at same conditions according to the procedure described in the literature.[32] In both the cases, double distilled aniline was used.

The PVB−PANI nanocomposite was prepared by solution processing. At room temperature, PVB was dissolved slowly in ethanol and PNF was added very slowly to this solution under stirring (5 wt %). After that, it was further stirred for another 3 h. Finally, it was poured to the X-band and Ku-band standard sample holders and kept in open air for drying (24 h). The PVB−PNF and PVB−PANI composites were named as PPNF and PP composites, respectively.

The surface morphology of the as-prepared PPNF nanocomposite was studied using a field-emission scanning electron microscope (Carl Zeiss). The relative permittivity ($\varepsilon_r$) of the prepared composites was recorded in the X-band and Ku-band using a vector network analyzer by the standard Nicholson−Ross−Weir method.[41]

## ASSOCIATED CONTENT

### Supporting Information

The Supporting Information is available free of charge on the ACS Publications website at DOI: 10.1021/acsomega.8b02037.

Power stimulated, absorbed, reflected, and lost in a conducting surface (PEC) for various thicknesses of the PPNF nanocomposite and the PP composite (PDF)

## AUTHOR INFORMATION


### Corresponding Author

*E-mail: onegroupb203@gmail.com (P.C.R.).

### ORCID

Praveen C. Ramamurthy: 0000-0003-2103-5600

Giridhar Madras: 0000-0003-2211-5055


### Notes

The authors declare no competing financial interest.

## ACKNOWLEDGMENTS

Authors gratefully acknowledge the technical support from MNCF (CeNSE), IISc, for this work.

## REFERENCES


(1) Wang, Y.; Chen, D.; Yin, X.; Xu, P.; Wu, F.; He, M. Hybrid of $MoS_2$ and Reduced Graphene Oxide: A Lightweight and Broadband Electromagnetic Wave Absorber. *ACS Appl. Mater. Interfaces* **2015**, *7*, 26226−26234.

(2) Bora, P. J.; Azeem, I.; Vinoy, K. J.; Ramamurthy, P. C.; Madras, G. Microwave Absorption Property of PVB-Polyaniline Nanocomposite. *Asia-Pacific Microwave Conference Proceedings*; APMC, 2018; pp 674−677.

(3) Zhang, Y.; Huang, Y.; Zhang, T.; Chang, H.; Xiao, P.; Chen, H.; Huang, Z.; Chen, Y. Broadband and Tunable High-Performance Microwave Absorption of an Ultralight and Highly Compressible Graphene Foam. *Adv. Mater.* **2015**, *27*, 2049−2053.

(4) Han, M.; Yin, X.; Li, X.; Anasori, B.; Zhang, L.; Cheng, L.; Gogotsi, Y. Laminated and Two-Dimensional Carbon-Supported Microwave Absorbers Derived from MXenes. *ACS Appl. Mater. Interfaces* **2017**, *9*, 20038−20045.

(5) Zhao, B.; Guo, X.; Zhao, W.; Deng, J.; Shao, G.; Fan, B.; Bai, Z.; Zhang, R. Yolk−Shell Ni@SnO2 Composites with a Designable Interspace To Improve the Electromagnetic Wave Absorption Properties. *ACS Appl. Mater. Interfaces* **2016**, *8*, 28917−28925.




DOI: 10.1021/acsomega.8b02037
*ACS Omega* 2018, 3, 16542−16548

(6) Zhao, B.; Guo, X.; Zhou, Y.; Su, T.; Ma, C.; Zhang, R. Constructing hierarchical hollow CuS microspheres via a galvanic replacement reaction and their use as wide-band microwave absorbers. *CrystEngComm* **2017**, *19*, 2178−2186.
(7) Deng, J.; Li, S.; Zhou, Y.; Liang, L.; Zhao, B.; Zhang, X.; Zhang, R. Enhancing the Microwave Absorption Properties of Amorphous CoO Nanosheet-Coated Co (Hexagonal and Cubic Phases) through Interfacial Polarizations. *J. Colloid Interface Sci.* **2018**, *509*, 406−413.
(8) Bora, P. J.; Porwal, M.; Vinoy, K. J.; Kishore; Ramamurthy, P. C.; Madras, G. Industrial Waste Fly Ash Cenosphere Composites Based Broad Band Microwave Absorber. *Composites, Part B* **2018**, *134*, 151−163.
(9) Qin, F.; Brosseau, C. A Review and Analysis of Microwave Absorption in Polymer Composites Filled with Carbonaceous Particles. *J. Appl. Phys.* **2012**, *111*, 061301.
(10) Ding, F.; Cui, Y.; Ge, X.; Jin, Y.; He, S. Ultra-Broadband Microwave Metamaterial Absorber. *Appl. Phys. Lett.* **2012**, *100*, 103506.
(11) Bora, P. J.; Vinoy, K. J.; Ramamurthy, P. C.; Kishore; Madras, G. Lightweight Polyaniline-Cobalt Coated Fly Ash Cenosphere Composite Film for Electromagnetic Interference Shielding. *Electron. Mater. Lett.* **2016**, *12*, 603−609.
(12) Bora, P. J.; Vinoy, K. J.; Ramamurthy, P. C.; Kishore; Madras, G. Electromagnetic Interference Shielding Effectiveness of Polyaniline-Nickel Oxide Coated Cenosphere Composite Film. *Compos. Commun.* **2017**, *4*, 37−42.
(13) Bora, P. J.; Mallik, N.; Ramamurthy, P. C.; Kishore; Madras, G. Poly(vinyl Butyral) -Polyaniline-Magnetically Functionalized Fly Ash Cenosphere Composite Film for Electromagnetic Interference Shielding. *Composites, Part B* **2016**, *106*, 224−233.
(14) Gooch, J. W.; Daher, J. K. *Electromagnetic Shielding and Corrosion Protection for Aerospace Vehicles*; Springer, 2007; pp 1−70.
(15) Kolev, S.; Yanev, A.; Nedkov, I. Microwave Absorption of Ferrite Powders in a Polymer Matrix. *Phys. Status Solidi C* **2006**, *3*, 1308−1315.
(16) Hwang, Y. Microwave Absorbing Properties of NiZn-Ferrite Synthesized from Waste Iron Oxide Catalyst. *Mater. Lett.* **2006**, *60*, 3277−3280.
(17) Liu, P.; Yao, Z.; Zhou, J.; Yang, Z.; Kong, L. B. Small Magnetic Co-Doped NiZn Ferrite/graphene Nanocomposites and Their Dual-Region Microwave Absorption Performance. *J. Mater. Chem. C* **2016**, *4*, 9738−9749.
(18) Khairy, M. Synthesis, characterization, magnetic and electrical properties of polyaniline/NiFe2O4 nanocomposite. *Synth. Met.* **2014**, *189*, 34−41.
(19) Lv, H.; Ji, G.; Liang, X.; Zhang, H.; Du, Y. A Novel Rod-like $MnO_2$@Fe Loading on Graphene Giving Excellent Electromagnetic Absorption Properties. *J. Mater. Chem. C* **2015**, *3*, 5056−5064.
(20) Fu, W.; Liu, S.; Fan, W.; Yang, H.; Pang, X.; Xu, J.; Zou, G. Hollow Glass Microspheres Coated with CoFe2O4 and Its Microwave Absorption Property. *J. Magn. Magn. Mater.* **2007**, *316*, 54−58.
(21) Bora, P. J.; Porwal, M.; Vinoy, K. J.; Ramamurthy, P. C.; Madras, G. Influence of MnO2decorated Fe Nano Cauliflowers on Microwave Absorption and Impedance Matching of Polyvinylbutyral (PVB) Matrix. *Mater. Res. Express* **2016**, *3*, 095003.
(22) Zong, M.; Huang, Y.; Zhang, N.; Wu, H. Influence of (RGO)/(ferrite) Ratios and Graphene Reduction Degree on Microwave Absorption Properties of Graphene Composites. *J. Alloys Compd.* **2015**, *644*, 491−501.
(23) Shu, R.; Li, W.; Zhou, X.; Tian, D.; Zhang, G.; Gan, Y.; Shi, J.; He, J. Facile preparation and microwave absorption properties of RGO/MWCNTs/ZnFe 2 O 4 hybrid nanocomposites. *J. Alloys Compd.* **2018**, *743*, 163−174.
(24) Yang, Z.; Wan, Y.; Xiong, G.; Li, D.; Li, Q.; Ma, C.; Guo, R.; Luo, H. Facile Synthesis of ZnFe2O4/reduced Graphene Oxide Nanohybrids for Enhanced Microwave Absorption Properties. *Mater. Res. Bull.* **2015**, *61*, 292−297.
(25) Zhao, H.; Cheng, Y.; Liang, X.; Du, Y.; Ji, G. Constructing Large Interconnect Conductive Networks: An Effective Approach for Excellent Electromagnetic Wave Absorption at Gigahertz. *Ind. Eng. Chem. Res.* **2018**, *57*, 2155−2164.
(26) Sarkar, D.; Bhattacharya, A.; Nandy, P.; Das, S. Enhanced Broadband Microwave Reflection Loss of Carbon Nanotube Ensheathed Ni-Zn-Co-Ferrite Magnetic Nanoparticles. *Mater. Lett.* **2014**, *120*, 259−262.
(27) Bora, P. J.; Azeem, I.; Vinoy, K. J.; Ramamurthy, P. C.; Madras, G. Morphology controllable microwave absorption property of polyvinylbutyral (PVB)-MnO 2 nanocomposites. *Composites, Part B* **2018**, *132*, 188−196.
(28) Zhuo, R. F.; Qiao, L.; Feng, H. T.; Chen, J. T.; Yan, D.; Wu, Z. G.; Yan, P. X. Microwave Absorption Properties and the Isotropic Antenna Mechanism of ZnO Nanotrees. *J. Appl. Phys.* **2008**, *104*, 094101.
(29) Tian, C.; Du, Y.; Xu, P.; Qiang, R.; Wang, Y.; Ding, D.; Xue, J.; Ma, J.; Zhao, H.; Han, X. Constructing Uniform Core-Shell PPy@PANI Composites with Tunable Shell Thickness toward Enhancement in Microwave Absorption. *ACS Appl. Mater. Interfaces* **2015**, *7*, 20090−20099.
(30) Cui, C.; Du, Y.; Li, T.; Zheng, X.; Wang, X.; Han, X.; Xu, P. Synthesis of Electromagnetic Functionalized Fe3O4 Microspheres/Polyaniline Composites by Two-Step Oxidative Polymerization. *J. Phys. Chem. B* **2012**, *116*, 9523−9531.
(31) Lakshmi, K.; John, H.; Mathew, K. T.; Joseph, R.; George, K. E. Microwave Absorption, Reflection and EMI Shielding of PU-PANI Composite. *Acta Mater.* **2009**, *57*, 371−375.
(32) Ramamurthy, P. C.; Mallya, A. N.; Joseph, A.; Harrell, W. R.; Gregory, R. V. Synthesis and Characterization of High Molecular Weight Polyaniline for Organic Electronic Applications. *Polym. Eng. Sci.* **2012**, *52*, 1821−1830.
(33) Bora, P. J.; Lakhani, G.; Ramamurthy, P. C.; Madras, G. Outstanding Electromagnetic Interference Shielding Effectiveness of Polyvinylbutyral-Polyaniline Nanocomposite Film. *RSC Adv.* **2016**, *6*, 79058−79065.
(34) Ates, M. A review on conducting polymer coatings for corrosion protection. *J. Adhes. Sci. Technol.* **2016**, *30*, 1510−1536.
(35) de Souza, S. Smart Coating Based on Polyaniline Acrylic Blend for Corrosion Protection of Different Metals. *Surf. Coating. Technol.* **2007**, *201*, 7574−7581.
(36) Huang, J.; Kaner, R. B. A General Chemical Route to Polyaniline Nanofibers. *J. Am. Chem. Soc.* **2004**, *126*, 851−855.
(37) Oyharçabal, M.; Olinga, T.; Foulc, M.-P.; Lacomme, S.; Gontier, E.; Vigneras, V. Influence of the Morphology of Polyaniline on the Microwave Absorption Properties of Epoxy Polyaniline Composites. *Compos. Sci. Technol.* **2013**, *74*, 107−112.
(38) Gupta, S.; Seethamraju, S.; Ramamurthy, P. C.; Madras, G. Polyvinylbutyral Based Hybrid Organic/inorganic Films as a Moisture Barrier Material. *Ind. Eng. Chem. Res.* **2013**, *52*, 4383−4394.
(39) Wu, M.; He, H.; Zhao, Z.; Yao, X. Electromagnetic and Microwave Absorbing Properties of Iron Fibre-Epoxy Resin Composites. *J. Phys. D Appl. Phys.* **2000**, *33*, 2398−2401.
(40) Bora, P. J.; Vinoy, K. J.; Ramamurthy, P. C.; Madras, G. Electromagnetic Interference Shielding Efficiency of $MnO_2$ nanorod Doped Polyaniline Film. *Mater. Res. Express* **2017**, *4*, 025013.
(41) Chen, L. F.; Chen, L. F.; Ong, C. K.; Ong, C. K.; Neo, C. P.; Neo, C. P.; Varadan, V. V.; Varadan, V. V.; Varadan, V. K.; Varadan, V. K. *Microwave Electronics Measurement and Materials Characterisation*; John Willy & Sons, 2004; pp 1−160.
(42) Lv, H.; Guo, Y.; Wu, G.; Ji, G.; Zhao, Y.; Xu, Z. J. Interface Polarization Strategy to Solve Electromagnetic Wave Interference Issue. *ACS Appl. Mater. Interfaces* **2017**, *9*, 5660−5668.
(43) Zhao, W.; Shao, G.; Jiang, M.; Zhao, B.; Wang, H.; Chen, D.; Xu, H.; Li, X.; Zhang, R.; An, L. Ultralight Polymer-Derived Ceramic Aerogels with Wide Bandwidth and Effective Electromagnetic Absorption Properties. *J. Eur. Ceram. Soc.* **2017**, *37*, 3973−3980.
(44) Huang, Y.; Wang, Y.; Li, Z.; Yang, Z.; Shen, C.; He, C. Effect of Pore Morphology on the Dielectric Properties of Porous Carbons for Microwave Absorption Applications. *J. Phys. Chem. C* **2014**, *118*, 26027−26032.


DOI: 10.1021/acsomega.8b02037
*ACS Omega* 2018, 3, 16542−16548